# REPORT DOCUMENTATION PAGE

Form Approved
OMB No. 0704-0188



| 1. REPORT DATE *(DD-MM-YYYY)* | 2. REPORT TYPE | 3. DATES COVERED *(From - To)* |
|---|---|---|
| | Technical Papers | |

**4. TITLE AND SUBTITLE**

Please see attached

**5a. CONTRACT NUMBER**

**5b. GRANT NUMBER**

**5c. PROGRAM ELEMENT NUMBER**

**6. AUTHOR(S)**

**5d. PROJECT NUMBER**
1011

**5e. TASK NUMBER**
0046

**5f. WORK UNIT NUMBER**
346204

**7. PERFORMING ORGANIZATION NAME(S) AND ADDRESS(ES)**

Air Force Research Laboratory (AFMC)
AFRL/PRS
5 Pollux Drive
Edwards AFB CA 93524-7048

**8. PERFORMING ORGANIZATION REPORT**

**9. SPONSORING / MONITORING AGENCY NAME(S) AND ADDRESS(ES)**

Air Force Research Laboratory (AFMC)
AFRL/PRS
5 Pollux Drive
Edwards AFB CA 93524-7048

**10. SPONSOR/MONITOR'S ACRONYM(S)**

**11. SPONSOR/MONITOR'S NUMBER(S)**
Please see attached

**12. DISTRIBUTION / AVAILABILITY STATEMENT**

Approved for public release; distribution unlimited.

**13. SUPPLEMENTARY NOTES**

**14. ABSTRACT**

20030116 044

**15. SUBJECT TERMS**

| 16. SECURITY CLASSIFICATION OF: | | | 17. LIMITATION OF ABSTRACT | 18. NUMBER OF PAGES | 19a. NAME OF RESPONSIBLE PERSON |
|---|---|---|---|---|---|
| | | | | | Leilani Richardson |
| a. REPORT | b. ABSTRACT | c. THIS PAGE | A | | 19b. TELEPHONE NUMBER *(include area code)* |
| Unclassified | Unclassified | Unclassified | | | (661) 275-5015 |

MEMORANDUM FOR PRR (Contractor/In-House Publication)

FROM: PROI (TI) (STINFO) 24 Jul 2000

SUBJECT: Authorization for Release of Technical Information, Control Number: **AFRL-PR-ED-TP-2000-155**
C. Johnson, S. Fallis, T. Groshens, K. Higa (NAWC); I. Ismail (ERC); T. Hawkins (AFRL/PRSP),
"Characterization of Nanometer- to Micron-Sized Aluminum Powders by Thermogravimetric Analysis"

**Journal of Material Research** **(Statement A)**
**(Submission Deadline: 31 July 00)**

**1.** This request has been reviewed by the Foreign Disclosure Office for: a.) appropriateness of distribution statement, b.) military/national critical technology, c.) export controls or distribution restrictions, d.) appropriateness for release to a foreign nation, and e.) technical sensitivity and/or economic sensitivity.
Comments:_____

Signature _____ Date _____

2. This request has been reviewed by the Public Affairs Office for: a.) appropriateness for public release and/or b) possible higher headquarters review.
Comments: _____

Signature _____ Date _____

**3.** This request has been reviewed by the STINFO for: a.) changes if approved as amended, b.) appropriateness of distribution statement, c.) military/national critical technology, d.) economic sensitivity, e.) parallel review completed if required, and f.) format and completion of meeting clearance form if required
Comments:_____

Signature _____ Date _____

4. This request has been reviewed by PR for: a.) technical accuracy, b.) appropriateness for audience, c.) appropriateness of distribution statement, d.) technical sensitivity and economic sensitivity, e.) military/ national critical technology, and f.) data rights and patentability
Comments:_____

APPROVED/APPROVED AS AMENDED/DISAPPROVED

_____

LAWRENCE P. QUINN DATE
Technical Advisor
Rocket Propulsion Division

# Characterization of nanometer- to micron-sized aluminum powders by thermogravimetric analysis

Curtis E. Johnson, Stephen Fallis, Thomas J. Groshens, and Kelvin T. Higa
*Chemistry and Materials Division, Research Department*
*Naval Air Warfare Center Weapons Division, China Lake, CA 93555-6100*

Ismail M. K. Ismail and Tom W. Hawkins
*Air Force Research Laboratory/~~PRSP~~ Propulsion Sciences Division*
*Edwards Air Force Base, CA 93524-7680*

***Keywords***: Nano-aluminum, ultrafine aluminum, BET, nitridation, oxidation, SEM, STM, TGA, X-ray diffraction.

## ABSTRACT

The reactivity of aluminum powders was studied by thermogravimetric analysis in air, oxygen, and nitrogen. Weight gains from complete oxidation of the aluminum were used to calculate particle sizes in the range of 30 nm to 500 nm. These particle sizes correlated well with particle sizes derived from surface area measurement. Particle size was also examined by scanning electron microscopy and atomic force microscopy, and compared to crystallite size determined by x-ray diffraction. Weight gains from complete oxidation were also used to determine the amount of active metal and aluminum oxide present in the submicron powders. Nitridation of aluminum powders was studied for extended times at 600°C. A 2-µm powder was nearly completely nitrided in 1 h, indicating that the nitride product has little inhibiting effect on the reaction.

## I. INTRODUCTION

Aluminum powders are used in a broad range of applications including rocket propellants, paints, and powder metallurgy processes for aircraft and automobile parts.[1] Since the reactivity of aluminum increases as the particle size decreases, small particles are desirable for aluminum used in propellants, explosives, and powder metallurgy processes. For example, use of ultrafine aluminum led to doubling the burn rate of a state of the art propellant.[2]

Commercially available aluminum powders are generally several microns or larger in size. Submicron aluminum powders have recently become available in limited quantities and sizes. As these powders are beginning to find their way into applications, there is a need to develop specifications and standard characterization procedures to ensure consistency of the material and its behavior. Key attributes of aluminum powders include particle size, size distribution, particle morphology, agglomeration, and aluminum oxide content.

Thermogravimetric analysis of submicron aluminum powders has been reported by a few groups to date,[3-5] including a preliminary report regarding some of the powders studied in this paper.[6] In the present paper, we explore the utility of thermogravimetric analysis in characterizing submicron aluminum powders and their reactivity to air and nitrogen.

## II. EXPERIMENTAL

The "ALEX" aluminum powder was obtained from The Argonide Corporation, the "LANL" powders were provided by Los Alamos National Laboratory, and the "H-2," "H-3," and "H-5" aluminum powders were obtained from Valimet. The remaining aluminum powders with CL- designations were prepared by a solution process, and passivated by slow exposure to air.[6-8] In the solution process, titanium isopropoxide was used as a catalyst. Most of the titanium was reduced and incorporated in the aluminum.[8] The molar ratio of catalyst to aluminum was: 0.1% for CL-01 and 40; 0.15% for CL-B, J, and K; 0.2% for CL-57; 0.5% for CL-06, 35, and 48; 2% for CL-10, 11, and 96; 3% for CL-41; and 10% for CL-49. After passivation of the aluminum in air, samples were dried as follows to remove organic contaminants: CL-57 was dried in air at room temperature, samples CL-B, J, and K were dried under vacuum at room temperature, and the remaining CL samples were dried under vacuum for about 30 min at 210°C, then cooled to room temperature before exposing to air.

Standard methods were used to hydrolyze aluminum powders and quantitatively measure the gas evolved.[9] Briefly, ~0.2 g samples were completely hydrolyzed in 1M NaOH aqueous solution. The weight percent of active aluminum in the sample was calculated based on the stoichiometry in Eq. (1):

$$Al + OH^- + 3H_2O = Al(OH)_4^- + 3/2H_2 \quad . \qquad (1)$$

Reported results are the average of three runs. Estimated accuracy is ±1%.

Scanning electron microscopy was conducted on an Electroscan Environmental Model E-3 in the presence of water vapor at about 5 torr, and an Amray Model 1400 instrument. X-ray powder diffraction patterns were obtained from petrolatum (Vaseline) mounted samples on glass slides using a Scintag PAD V diffractometer with Cu $K_\alpha$ radiation. Average crystallite sizes were calculated from X-ray line widths using the Scherrer equation.[10] Reported values are the average of four sizes calculated from peaks at $2\theta = 38$, 44, 65 and 78°.

Samples were prepared for atomic force microscopy analysis by dispersing in ethanol by sonication. A drop of the solution was placed on the sample holder, then allowed to dry. A Digital Instrument's Nanoscope III AFM was used to image the sample in air. An F head (21 micron scan range) was utilized along with a 200 micron cantilever. The cantilever was scanned at a rate of 1.57 Hz in constant cantilever deflection mode of operation.

Thermogravimetric analysis (TGA) in flowing air and oxygen (99.995% purity) was conducted on a TA Instruments 2950 Thermogravimetric Analyzer with a DuPont 2100 Thermal Analyst controller. The highest temperature used in these experiments was 950°C due to the 1000°C limit of the instrument. Sample weights ranged from 1-5 mg and weight data were corrected for the instrumental baseline response, based on blank (empty aluminum oxide pan) experiments conducted periodically.

For thermogravimetric analysis under nitrogen, the isothermal increase in sample weight was monitored as a function of time at ambient pressure. The TGA apparatus is shown in Figure 1 with its four main components: a CAHN-2000 electrobalance with a cylindrical quartz sample container (bucket) suspended on the balance beam, a vertical furnace surrounding the reactor, a roughing pump attached to an oil diffusion pump with a cryogenic stack, and a set of three MKS® transducer heads (1, 10 and 1000 Torr). To start a run, a small weight of the powder, normally 12-15 mg, was placed in the quartz bucket, suspended on the balance beam, and evacuated to $10^{-6}$ torr for two hours. The sample was brought to ambient pressure using ultrahigh pure nitrogen (>99.999% purity) at atmospheric pressure for 30 min. The concentration of impurities in the nitrogen stream, as supplied by the manufacturer, was as follows: 0.382 ppm moisture, 0.5 ppm oxygen, 0.1 ppm total hydrocarbons, < 1 ppm $CO_2$ and < 1 ppm CO. Samples were heated at 35°C/min to an isothermal temperature of 600°C under a constant nitrogen flow rate of 50 cc/min. The increase in sample weight, attributed to the reaction $2Al + N_2 \rightarrow 2AlN$, was followed with time. The increase in weight was monitored as a function of time until the weight increase became insignificant or when sample weight remained practically constant.

The surface area of aluminum powders was determined by conventional volumetric gas adsorption technique using a Micromeritics Digisorb 2600 surface area analyzer. Before each measurement, the powder was evacuated for 24 hours at 250°C. This treatment removed the foreign species adsorbed at the surface such as $CO_2$, moisture, oils and grease. After the pretreatment, the evacuated samples were immersed in a liquid nitrogen bath and the adsorption isotherms of nitrogen at -196°C were obtained. The isotherms on all powders were of Type II, indicating that the aluminum powders examined here are typical non-porous materials.[11] To calculate the surface area from the isotherms, the Brunauer, Emmett and Teller (BET) equation was used.[12]

## III. RESULTS AND DISCUSSION

The aluminum powders characterized in this work originated from four distinct preparation processes: (1) a solution process involving the catalyzed decomposition of trialkyl amine adducts of alane ($AlH_3$) at 40-80°C (samples with CL- designations),[6-8] (2) an electroexplosion process using aluminum wire ("ALEX"), (3) a vapor condensation process ("LANL"), and (4) a gas atomization process (H- designations). All of the methods are capable of producing a range of particle sizes, but the first three methods readily produce nanosized particles, while gas atomization produces mainly micron-sized and larger particles. Figure 2 shows micrographs from scanning electron microscopy (SEM) of representative powders. Particle size and morphology from SEM and atomic force microscopy (AFM) data are collected in Table I. For SEM, the most common particle size is given in Table I, along with the range of sizes observed. With AFM, the presence of electrostatic charges near ultrafine aluminum samples caused difficulties and prohibited obtaining valid views of some samples in this investigation. The particle size given in Table I is the average size or the range of sizes observed. The solution and vapor condensation processes tend to give a narrow particle size range, often varying by a factor of about 3. The particle size generally varies by a factor of 20 or more for the electroexplosion and gas atomization processes. Powders prepared by the solution process tend to be tightly agglomerated into small clumps, with the larger sizes exhibiting particles that are fused together (Figs. 2d-2f). The other three methods produced loosely agglomerated particles where the clumps can be readily separated physically.

### A. Thermogravimetric Analysis in Air and Oxygen → bump title to next page

Figures 3 and 4 show TGA data in air for some of the powders. All of the powders show an initial weight loss due to loss of volatile components (e.g., water and organics) upon heating to about 350°C. Each TGA curve is normalized to the minimum weight that was reached between the loss of volatiles and the weight gain due to aluminum oxidation. The oxidation proceeds in two distinct steps separated by slow oxidation from about 600 to 700°C. The melting of aluminum at 660°C appears to have no immediate effect on the oxidation rate (see Fig. 4 for an expanded view in this region). The oxidation rate increases above 700°C, reaching a maximum between 750 and 850°C. Submicron powders are completely or nearly completely oxidized after several hours heating at 850°C. Complete oxidation is indicated by reaching a constant weight and by the color of the residue, which is white when oxidation is complete, but noticeably gray if a small amount (about 1%) of unoxidized aluminum remains. The weight gained in the first step depends markedly on the particle size, with the smallest powders giving the largest weight gain below 700°C. Further analysis of intermediate stages of the oxidation process is presented in Section C.

Sample CL-B exhibits a relatively large weight loss due to the presence of residual organics that were not removed by drying under vacuum at room temperature. When a larger weight of sample CL-B was used in the TGA experiment, rapid oxidation initiated at 588°C, ascribed to ignition of the aluminum (dashed curve in Fig. 4). This ignition or runaway oxidation phenomenon was often observed for the smaller sized powders when larger sample amounts were used. When ignition occurred, the oxidation rate increased about ten-fold for the first oxidation step, but subsequent oxidation occurred at a much slower rate, leaving a gray residue after several hours of heating at 850°C. These results are interpreted in terms of rapid melting of the aluminum upon ignition, with formation of relatively large droplets of molten aluminum that are slow to oxidize. Ignition could usually be avoided by using very small sample sizes (about 1 mg) spread out in the sample pan. A more reliable approach was to reduce the heating rate from 20°C/min to 3°C/min. This eliminated ignition and allowed for larger sample sizes.

We also observed the runaway oxidation of ALEX aluminum when a 10 mg sample was heated at 25°C/min. The final weight gain after heating at 1050°C for 1000 min was only 57%, compared to a 75% weight gain for material heated to 950°C for 240 min where runaway oxidation did not occur (4 mg sample with a heating rate of 3°C/min in the range of 350-600°C). The reduced weight gain was not attributable to extensive nitridation of the aluminum, since x-ray diffraction of the product showed weak peaks for aluminum nitride compared to intense aluminum oxide peaks, with a significant amount of elemental aluminum also present.

The weight gain observed on complete oxidation was used to calculate the weight percent of active aluminum in the sample. For this calculation the samples are assumed to consist of only unreacted aluminum and aluminum oxide at the point of minimum weight. The subsequent

weight gain is ratioed to the theoretical weight gain of pure aluminum converting to $Al_2O_3$, where the weight increases by 88.95%. The weight changes for the aluminum samples are listed in Table II (columns 2 and 3), along with the calculated weight percent of active aluminum (column 4). Based on the same assumptions, the weight percent oxygen is also calculated for each sample (see Table II, column 4).

To check for possible nitridation of the aluminum, oxidation was conducted in pure oxygen. Figure 5 shows TGA curves of sample CL-35 heated in air and oxygen. The TGA curves are identical, so there is no evidence for nitridation during heating in air. Conversion of aluminum to AlN results in a weight increase of only 51.91%, compared to 88.95% for $Al_2O_3$. Since the weight gains under air and oxygen are the same throughout the oxidation process, the rate of oxidation is the same in air and pure oxygen.

The weight percent active aluminum was also determined by hydrolysis of the aluminum, with quantitative determination of the gas evolved. The results are listed in Table III, with the corresponding values from TGA data listed for comparison. The TGA values in Table III are based on the material before loss of volatiles during heating, and therefore differ slightly from the values in Table II. Excellent agreement between the two methods are found for four samples, while the three smaller China Lake powders gave lower active metal contents by the TGA method. For the ALEX powder, the active metal content from hydrolysis, 86.0%, is close to the TGA result of >83.6%, where the oxidation was not quite complete (the residue had a dull white coloration, compared to bright white for completely oxidized samples).

The weight gain upon complete oxidation of the aluminum was also used to calculate an average particle size. For this calculation the powders were assumed to have an oxide coating equivalent to 2.5 nm of fully dense $Al_2O_3$. Reported values for the thickness of the native oxide layer on aluminum exposed to air range from about 2 to 4 nm.[3] An oxide thickness of 2.5 nm was determined by transmission electron microscopy on LANL samples. Particle sizes were calculated based on uniform spherical particles according to

$$F_{Al}/F_{obs} - 1 = (d_{Al_2O_3}/d_{Al})[(x/(x-2t))^3 - 1] \ , \qquad (2)$$

where $F_{Al}$ is the fractional weight gain for oxidation of pure Al to $Al_2O_3$ (0.88946), $F_{obs}$ is the observed fractional weight gain from the minimum weight to the final weight, x is the particle diameter, and t is the oxide layer thickness (taken as 2.5 nm). Note that $F_{obs}/F_{Al}$ is the weight fraction of active Al that is given as a percentage in Table II, column 4. The density of Al and $Al_2O_3$ were taken as 2.702 and 3.97, respectively. The calculated TGA sizes represent a weight- or volume-weighted average particle size. Inspection of Eq. (2) shows that the calculated TGA size is directly proportional to the assumed oxide thickness.

The TGA particle sizes are shown in Figure 3 and in column 5 of Table II. The TGA particle sizes are generally consistent with the SEM and AFM particle sizes shown in Table I. Figure 6 shows how the particle size relates to the weight percent active aluminum using Eq. (2) and assuming a constant 2.5 nm oxide thickness for all particle sizes. The curve gives the calculated dependence, while specific materials are placed on the curve according to the TGA results. For ALEX and H-2, where oxidation was incomplete, the hydrolysis result for weight percent active Al in Table III was used. The corresponding sizes, based on Eq. (2), are 157 nm and 2.4 μm for ALEX and H-2, respectively. Figure 6 shows that the active aluminum content drops rapidly as the particle size falls below 100 nm. For energy producing applications a tradeoff exists between enhanced reactivity and reduced energy content. This tradeoff could be mitigated by using unpassivated submicron aluminum powders which are pyrophoric, or possibly by developing alternatives to oxide passivation of the aluminum.

**B. Surface Area Measurement and Comparison of Particle Size Determinations**

The data obtained from gas adsorption are listed in Table II. The sixth and seventh columns list the values of surface area, $A_s$, computed from the two runs conducted for each sample. Assuming that the particles are spherical, the following equation was used to estimate the BET average particle size $d$:

$$As\ (m^2/g) = \frac{6}{\rho\ (g/cc) \times d\ (microns)} \qquad (3)$$

where $\rho$ is the density of particles (taken here as 2.702 g/cc for aluminum), and the average of the two $A_s$ values was used. The BET average particle sizes are listed in Table II, and are within the size range obtained by SEM and AFM (see Table I) for most samples.

Particle size data from BET, SEM, and TGA data are presented graphically in Figure 7, along with average crystallite sizes determined by x-ray diffraction (XRD). The TGA and BET sizes correlate very well, with the TGA size generally slightly larger than the BET size. This confirms that the TGA method gives a useful measure of particle size. The TGA and BET sizes show a fair correlation with the SEM sizes. Assigning a single particle size based on SEM micrographs is somewhat subjective, and complicated by agglomeration of particles, by the distribution of particle sizes, and by image resolution limitations for particle sizes below 100 nm. The average crystallite size correlated well with particle sizes for the LANL and ALEX materials. For the China Lake samples, the crystallite size exhibited a much narrower range than the particle sizes.

This indicates that, for the larger particles, either renucleation occurred on the surface of growing particles, or many separate particles combined together.

### C. Calculation of Aluminum Thickness Oxidized in TGA Experiments

The controlled oxidation of aluminum in the TGA experiments can be interpreted as the growth of an increasingly thick layer of aluminum oxide around a shrinking core of aluminum. Based on this model, an attempt was made to estimate the thickness of aluminum converted to oxide at various stages of the TGA experiment. Samples that appeared to have relatively narrow size distributions (from SEM and TGA data) were chosen for this analysis. The weight gained at three stages of heating was tabulated, and the corresponding thickness of aluminum oxide was calculated. The results are summarized in Table IV and Figure 8. For the first oxidation step, the weight increased up to the point where the oxidation rate minimized (near the melting point). For all five submicron samples analyzed, this corresponded to 12 -15 nm of Al oxidized (see the first 5 values in column 6 of Table IV ). The thickness includes the original 2.5 nm $Al_2O_3$ layer. By similar analysis of the data in columns 7 and 8 of Table IV, the average total thickness of Al oxidized was about 90 nm for the second oxidation stage and about 300 nm for the third oxidation stage. Based on these values, the particle size that would be 99% converted to oxide was calculated. The observation of a kinetically limiting oxidation reaction and limited oxide growth at high temperature is well documented in the literature. Typically, the oxide thickness on smooth flat surfaces is 17-21 nm [Reference?]. This compares very favorably with the results reported here in Table IV, 13-23 nm with an average value of 18 nm. Theoretically, a 15 nm-thick Al yields an oxide thickness of ~18 nm, as shown in Table IV.

The last three samples in Table IV do not conform to the patterns of oxidation established above. The ALEX sample exhibited the expected extent of oxidation in the first step, but much less oxidation in the second and third stages. This is readily explained by the presence of some micron sized particles as seen by SEM. The larger particles have considerable limitation to diffusion of oxygen molecules, the oxidation reaction on these particles was not completed. Thus, the presence of relatively large particles is easily apparent from the calculations developed here.

Although sample CL-49 has a very small particle size, 23 nm, the oxidation was slow, and the corresponding calculated thickness was small (columns 6 and 7 of Table 4). This indicates that the sample contains an impurity that either reduces the weight gain (causing an artificially low calculated particle size) or inhibits the oxidation reaction. Sample CL-49 contains about 10 wt mol % Ti that could be inhibiting the reaction via the formation of oxidation resistant titanium

aluminide. Sample CL-10 also has a larger particle size distribution than most of the samples examined by SEM. It exhibits a behavior intermediate between that of ALEX and CL-49 during the three stages of oxidation. This sample should be characterized further to check for impurities.

Thus, the results on the oxidation of aluminum powders indicate that TGA data can be useful in qualitatively examining particle size distributions, and provide evidence of possible impurities.

### D. Thermogravimetric Analysis in Nitrogen

The nitridation of aluminum powders was studied isothermally at 600°C by TGA, expanding on previous work on an ALEX sample and a 6-μm gas atomized powder.[4] In the previous study, the 6-μm powder exhibited a maximum weight gain of only 7.8% after about 2500 min at 600°C. This result was interpreted in terms of a 147 nm limiting thickness of AlN surrounding the particle, which strongly inhibited further reaction. The smaller ALEX material, with a BET size of 183 nm, exhibited a 47.3% weight gain after about 5400 min at 600°C, indicating that the nitridation reaction was not limited for this material.

Figures 9 and 10 display results of TGA experiments under nitrogen for the current group of powders. The maximum weight gain is given in Table II, column 9, with the expected maximum weight gain, based on the active metal content, given in column 10. The most surprising result is the rapid and nearly complete nitridation of the H-2 powder, shown in Figure 9. For comparison, in air H-2 Al gained only 7 wt. % upon heating at 600°C for 900 min. The second largest powder studied, CL-40 (TGA size 460 nm), also exhibited rapid and extensive nitridation. In contrast, the third largest powder studied, CL-40 (TGA size 256 nm) was the slowest to react and gave by far the lowest maximum weight gain. The smaller powders gave somewhat scattered results, but all ultimately gave maximum weight gains that were larger than expected. Sample CL-35 was run for 28000 min, giving a maximum weight gain of 55%, which is higher than the theoretical value of 51.9% for pure Al.

The residues from nitridation of samples CL-41 and CL-35 were analyzed by XRD. The diffraction pattern in Figure 11 for the CL-41 residue shows mainly the hexagonal AlN phase, some unreacted Al, and possibly aluminum oxy-nitride phases that may be associated with weak peaks in the pattern. ~~Aluminum oxide phases cannot be ruled out since they tend to be amorphous when formed under similar conditions in air.~~ The results indicate that aluminum ~~oxide or~~ oxy-nitride phases are formed, especially at longer times in the TGA experiment. Traces of oxygen or water in the system apparently react with the aluminum or with the AlN product. Thermodynamics dictate that any available oxygen in the system should form aluminum oxide,

since the conversion of AlN + $O_2$ to $Al_2O_3$ + $N_2$ is favored by 489 kJ/mol Al at 600°C, while the conversion of AlN + $H_2O$ to $Al_2O_3$ + $NH_3$ is favored by 152 kJ/mol Al.

## IV. CONCLUSIONS

Thermogravimetric analysis of submicron aluminum powders in air provides quantitative information on active metal content and particle size, and qualitative information on particle size distribution. Particle sizes calculated from TGA data correlate well with particle sizes derived from surface area measurement by gas adsorption. This correlation is reasonable since the TGA size is based on the weight fraction of the aluminum oxide passivation layer that covers the surface of the particles. In contrast to oxidation, nitridation at 600°C proceeded with less inhibiting effect of the aluminum nitride product on the reaction.

## ACKNOWLEDGMENTS

C. J. thanks Richard Scheri, Michael Dowd, Dan Kline, and John Johnson for SEM characterization, and Brian Zentner for synthesis of aluminum powders. We also thank Chris Aumann and Joe Martin for providing the LANL aluminum powder and communicating unpublished results. The work at China Lake was supported by the SERDP Green Missile program, by the Office of Naval Research (J. Goldwasser, R. Carlin, and J. Chew), and by the Naval Air Warfare Center Core Science and Technology program.

I. I. And T. H. thank Ms. Diane Hagler, Dr. Robert Stanley and Mr. Mark Feathers at Redstone Arsenal (AAMICOM) for their support of this work in the SERDP Green Missile program. This work was also supported, in part, by of the Propulsion Directorate of the Air Force Research Laboratory, Edwards Air Force Base. Special appreciation goes to Dr. Kevin Chaffee for the X-ray diffraction work, to Ms. Marietta Fernandez for AFM work, to Mr. Paul Jones for TGA work, and to Mr. Adam Brand and Mr. Milton McKay for their technical support and stimulating discussions.

## REFERENCES

1. T. B. Gurganus, Adv. Mater. Process. **148**, 57-59 (1995).
2. F. Pickett and D. Booth, in *Proceedings of the 1995 JANNAF Propulsion and Joint Subcommittees Meeting,* Tampa, FL, 4-8 December 1995.
3. C. E. Aumann, G. L. Skofronick, and J. A. Martin, J. Vac. Sci. Technol. B **13**, 1178-1183 (1995). journal titles are italicized
4. I. M. K. Ismail and T. W. Hawkins, "Evaluation of Electro-exploded Aluminum (ALEX) for Rocket Propulsion", CPIA Publication 650, **2**, 25-39 (1996).
5. M. M. Mench, K. K. Kuo, C. L. Yeh, and Y. C. Lu, Combust. Sci. and Tech. **135**, 269-292 (1998).
6. C. E. Johnson and K. T. Higa in *Nanophase and Nanocomposites Materials II,* edited by S. Komarneni, J. C. Parker, H. J. Wollenberger (Mater. Res. Soc. Symp. Proc. **457**, Warrendale, PA, 1997).
7. K. T. Higa, C. E. Johnson, and R. A. Hollins, U.S. Patent No. 5 885 321 (23 March 1999).
8. C. E. Johnson, unpublished results. Details on the synthesis of the China Lake powders will be provided in a separate publication.
9. H. C. Brown, *Organic Synthesis via Boranes,* (Wiley, New York, 1975).
10. H. P. Klug and L. E. Alexander, *X-ray Diffraction Procedures for Polycrystalline and Amorphous Materials,* 2nd ed., (Wiley, New York, 1974), p. 687.

11. S. J. Gregg and K. S. Sing, *Adsorption, Surface Area and Porosity,* 2nd ed., (Academic Press, New York, 1982).
12. S. Brunauer, P. H. Emmett and E. Teller, J. Am. Chem. Soc. **60**, 309 (1938).

italics

TABLE I. Characterization of aluminum powders by SEM, AFM, and XRD.

| Sample | SEM size (range) (nm) | SEM particle morphology | AFM size (nm) | XRD size (nm) |
|---|---|---|---|---|
| Valimet H-2 | --- (200-8000) | loosely agglom. | 500-3500 | 580 |
| CL-57 | 1000 (800-1500) | highly fused | --- | 140 |
| CL-40 | 300 (150-400) | highly fused | --- | 105 |
| CL-01 | 300 (150-350) | highly fused | 260 | 104 |
| CL-35 | 200 (125-300) | fused | --- | 120 |
| CL-06 | 250 (100-350) | highly fused | --- | 109 |
| ALEX 72095 | 150 (50-5000) | loosely agglom. | 175 | 173 |
| CL-48 | 125 (75-250) | fused | --- | 93 |
| CL-10 | ~100 (50-300) | highly fused | --- | 62 |
| CL-11 | 120 (100-200) | agglomerated | 175 | 68 |
| CL-96 | 100 (80-150) | agglomerated | 130 | 72 |
| CL-41 | 150 (70-200) | agglomerated | 30-110 | 70 |
| CL-49 | 120 (60-200) | agglomerated | --- | 67 |
| LANL RF-A | 60 (~40-100) | loosely agglom. | 40-120 | 40 |

TABLE II. Characterization of aluminum powders by TGA and BET.

| Sample | % volatiles by TGA | % Wt. gain in air[a] | Wt. % active Al (% O) | TGA size (nm) | Surface area ($m^2/g$) | | BET size (nm) | % Wt. gain in $N_2$, 600°C | % Wt. gain in $N_2$ expected |
|---|---|---|---|---|---|---|---|---|---|
| Valimet H-2 | 0.2 | 78.2[b] | --- | --- | 2.16 | 2.12 | 1035 | 48.5 | 51.3[d] |
| CL-57 | 1.6 | 60.26[b] | --- | --- | --- | --- | --- | --- | --- |
| CL-40 | 0.4 | 84.77[c] | 95.3 (2.2) | 460 | 7.31 | 6.42 | 322 | 42.8 | 49.5 |
| CL-J | 0.5 | 83.60 | 94.0 (2.8) | 355 | --- | --- | --- | --- | --- |
| CL-01 | 1.8 | 81.64 | 91.9 (3.8) | 256 | 10.6 | 10.7 | 209 | 26 | 47.7 |
| CL-35 | 1.7 | 79.75 | 89.6 (4.9) | 201 | 16.88 | 14.58 | 141 | 55 | 46.5 |
| CL-06 | 1.9 | 79.27[c] | 89.1 (5.1) | 190 | --- | --- | --- | --- | --- |
| ALEX 72095 | 1.1 | 75.12[b] | >84.5[b] (<7.3) | >130[b] | 13.4 | 13.2 | 167 | 47 | 45.1[d] |
| CL-48 | 2.2 | 75.84 | 85.3 (6.9) | 138 | --- | --- | --- | --- | --- |
| CL-10 | 3.1 | 70.24 | 79.0 (9.9) | 93 | --- | --- | --- | --- | --- |
| CL-B | 10.4 | 69.04 | 77.6 (10.5) | 86 | --- | --- | --- | --- | --- |
| CL-11 | 1.9 | 65.93 | 74.1 (12.2) | 73 | 55.2 | 55.6 | 40 | 43 | 38.5 |
| CL-96 | 6.2 | 64.32 | 72.2 (13.1) | 67 | 53.3 | 53.9 | 41 | 47 | 37.5 |
| CL-41 | 5.5 | 63.04 | 70.9 (13.7) | 63 | 79.6 | 78.3 | 28 | 40.4 | 36.8 |
| LANL RF-A | 4.3 | 56.98 | 64.0 (16.9) | 49 | 48.6 | 47.6 | 46 | 43.2 | 33.2 |
| CL-K | 10.4 | 54.59 | 61.4 (18.2) | 45 | --- | --- | --- | --- | --- |
| LANL-1 | 3.7 | 52.40 | 58.9 (19.3) | 41 | --- | --- | --- | --- | --- |
| LANL RF19 | 4.1 | 46.16 | 51.9 (22.6) | 33 | --- | --- | --- | --- | --- |
| CL-49 | 20.9 | 33.77 | 39±2 (27.9) | ~23 | --- | --- | --- | --- | --- |
| IH-1 | 10.0 | 19.93 | 22.4 (36.6) | 15 | --- | --- | --- | --- | --- |

[a]The percent weight gain is computed from the final weight (typically after 4 h at 850°C) and the minimum weight reached at 300-350°C.

[b]Oxidation incomplete. The H-2 sample was heated for 8 h at 850°C and 2 h at 950°C (after 4 h at 850°C, the weight gain was 61.02%). The ALEX sample was heated for 4 h at 950°C to give nearly complete oxidation (after 4 h at 850°C, the weight gain was 70.85%).

[c]Sample CL-40 was heated for 16 h at 850°C to give complete oxidation (after 4 h at 850°C, the weight gain was 83.43%). Sample CL-06 was heated for 8 h at 850°C to give complete oxidation (after 4 h at 850°C, the weight gain was 78.66%).

[d]Based on the wt. % active Al from Table III, column 2.

TABLE III. Comparison between weight percent of active aluminum metal as determined by the hydrolysis method and TGA data.

| Sample | Wt. % active metal from hydrolysis | Wt. % active metal from TGA |
|---|---|---|
| Valimet H-2 | 98.9 | --- |
| CL-40 | 94.5 | 94.9 |
| ALEX 72095 | 86.0 | >83.6 |
| CL-48 | 84.0 | 83.4 |
| CL-10 | 80.7 | 76.6 |
| CL-41 | 72.1 | 67.0 |
| LANL RF-A | 61.8 | 61.2 |
| CL-49 | 35.1 | 31±2 |

TABLE IV. Calculation of total thickness of aluminum oxidized for three stages of heating in air.

| Sample | Particle size (nm)[a] | First Stage % of total wt. gained during first step, ~600°C[b] | Second Stage % of total wt. gained after 10 min at 850°C | Third Stage % of total wt. gained after 4 h at 850°C | Al thickness oxidized on heating to 600°C (nm) | Al thickness oxidized after 10 min at 850°C (nm) | Al thickness oxidized after 4 h at 850°C (nm) |
|---|---|---|---|---|---|---|---|
| LANL RF-A | 49 | 85.4 | 100.0 | 100.0 | 12.5 | complete | complete |
| CL-48 | 138 | 42.5 | 99.6 | 100.0 | 13.3 | 59 | complete |
| CL-35 | 201 | 28.9 | 98.2 | 100.0 | 12.6 | 76 | complete |
| CL-01 | 256 | 26.6 | 83.5 | 100.0 | 14.4 | 59 | complete |
| CL-40 | 460 | 16.0 | 68.8 | 98.4 | 14.9 | 76 | 175 |
| Valimet H-2[c] | ~2000 | 6.3 | 26.7 | 69.4 | 23 | 100 | 325 |
| Valimet H-3[c] | ~3000 | 3.3 | 17.6 | 50.2 | 17 | 96 | 310 |
| Valimet H-5[c] | ~5000 | 1.8 | 9.5 | 34.0 | 19 | 81 | 325 |
| CL-49 | ~23 | 23.9 | 96.6 | 100.0 | 2.8 | 7 | complete |
| CL-10 | 93 | 34.5 | 75.3 | 100.0 | 7.9 | 19 | complete |
| ALEX 72095 | 157 | 37.9 | 81.8 | 91.6 | 13.3 | 35 | 45 |

[a]Particle sizes are the values determined by TGA, except for the Valimet samples where the nominal size is given, and ALEX where the value is based on the wt. % active Al determined by hydrolysis.

[b]The TGA temperature program for most experiments was: heat at 20°C/min to 350°C, then 3°C/min to 600°C, then 20°C/min to 850°C. For samples Valimet H-3 and Valimet H-5, the temperature program was: heat at 20°C/min to 850°C. The first step weight gain was taken where the oxidation rate was a minimum (588-599°C for the first heating program, 691°C for the second heating program). The oxidation rate becomes very low at this point, and the two different heating programs gave nearly identical weight gains at the stages given here.

[c]For samples H-2, H-3, and H-5, the total weight gained for complete oxidation, used to calculate the values in columns 3-5, is taken as the expected value for the nominal particle size with a 2.5 nm oxide thickness, i.e., 87.97, 88.29, and 88.55% for 2, 3, and 5 μm particles, respectively.

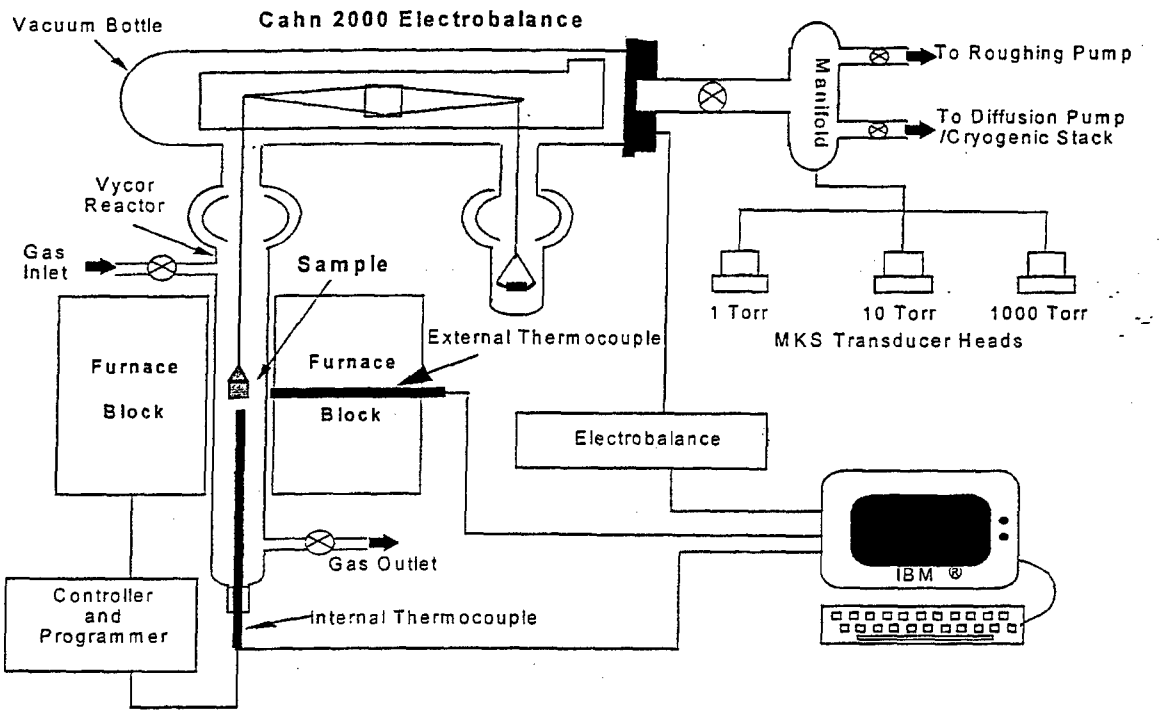


FIG 1. TGA apparatus used for experiments conducted under nitrogen atmosphere.

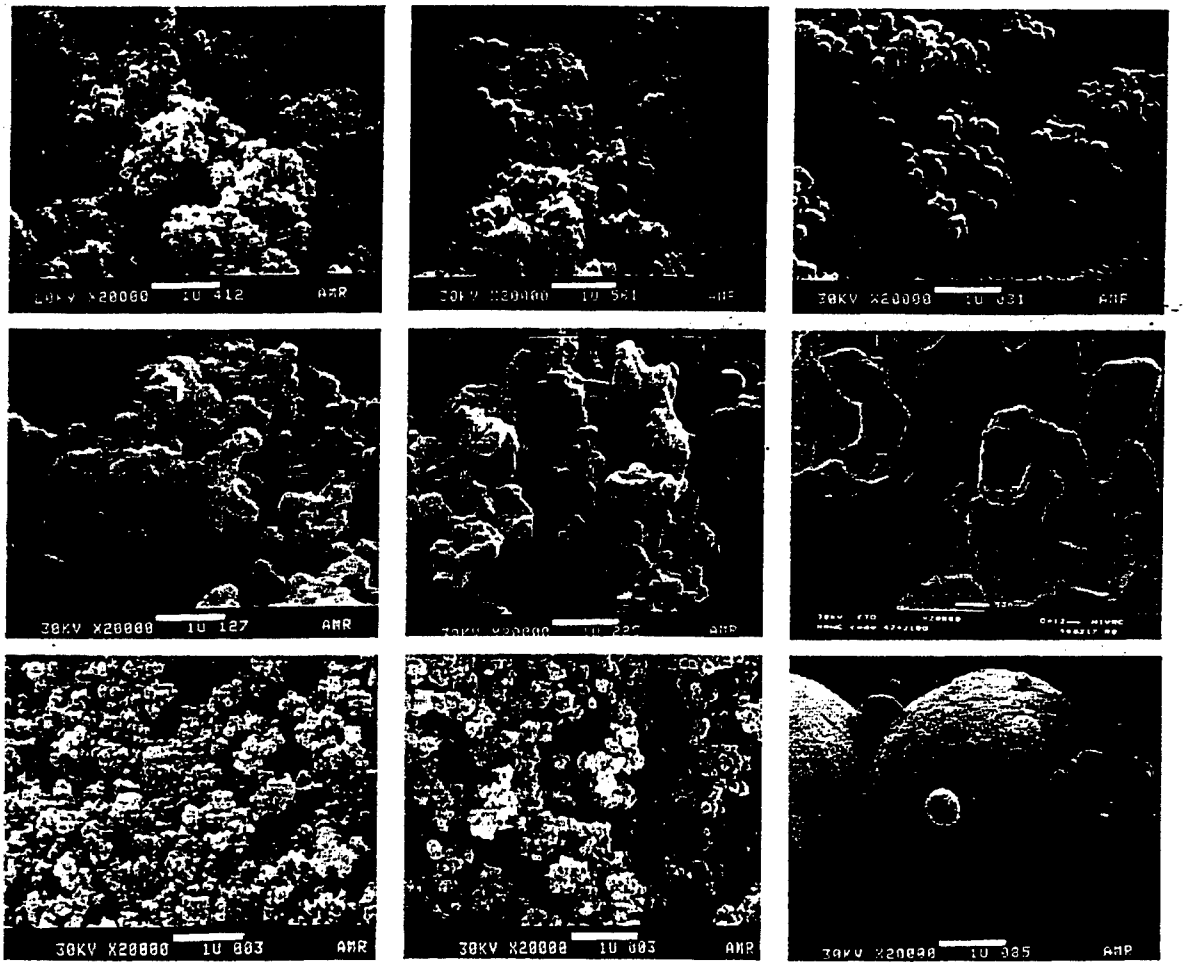


FIG 2. SEM micrographs of aluminum powders at 20,000X magnification:
Top row: samples CL-11, CL-10, CL-35
Middle row: CL-01, CL-40, CL-57
Bottom row: LANL-1, ALEX 72095, H-2.

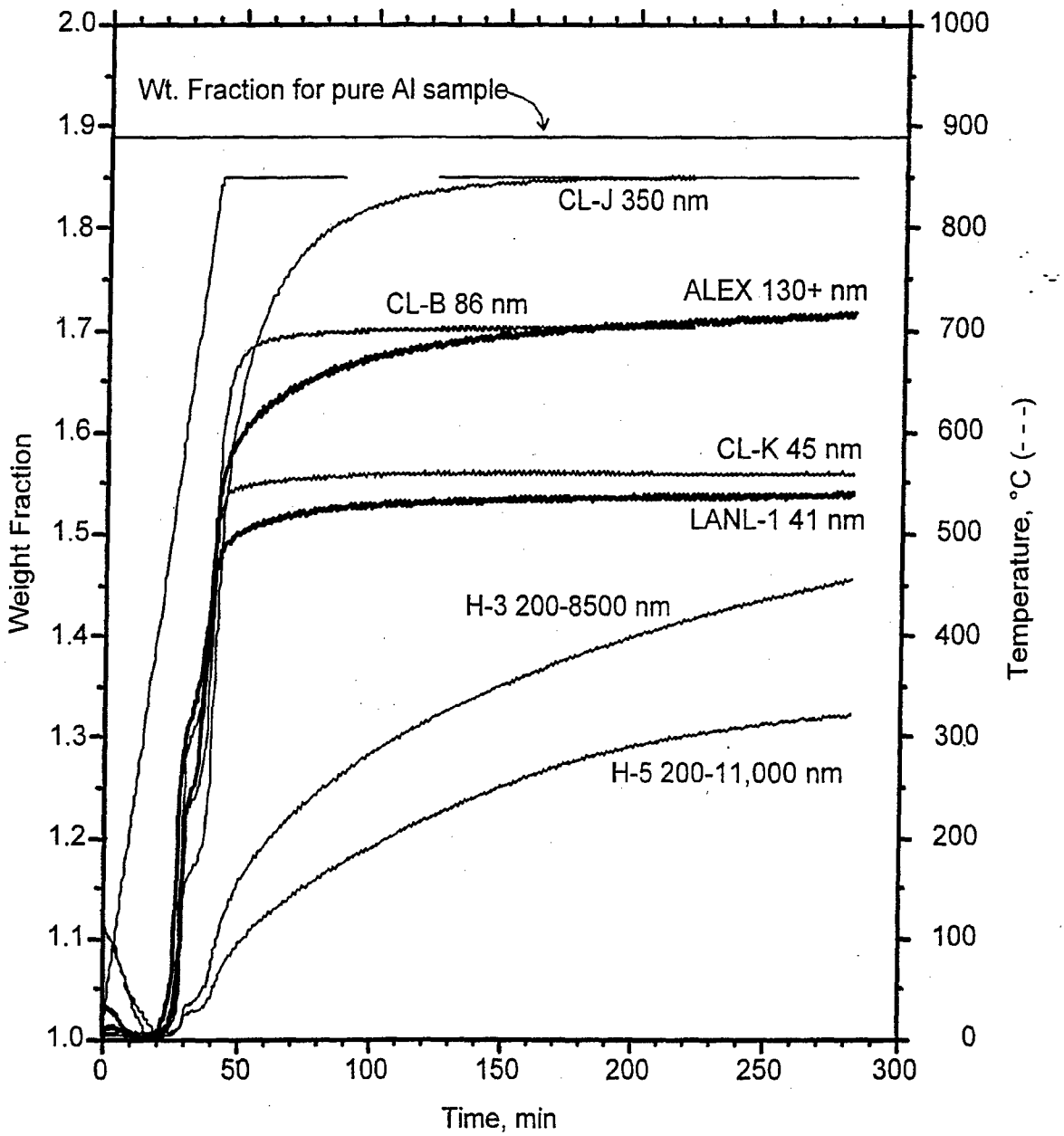


FIG. 3. TGA of aluminum powders oxidized in air. Samples were heated at 20°C/min to 850°C, then held at 850°C for four hours. The sample weight was normalized to the minimum weight.

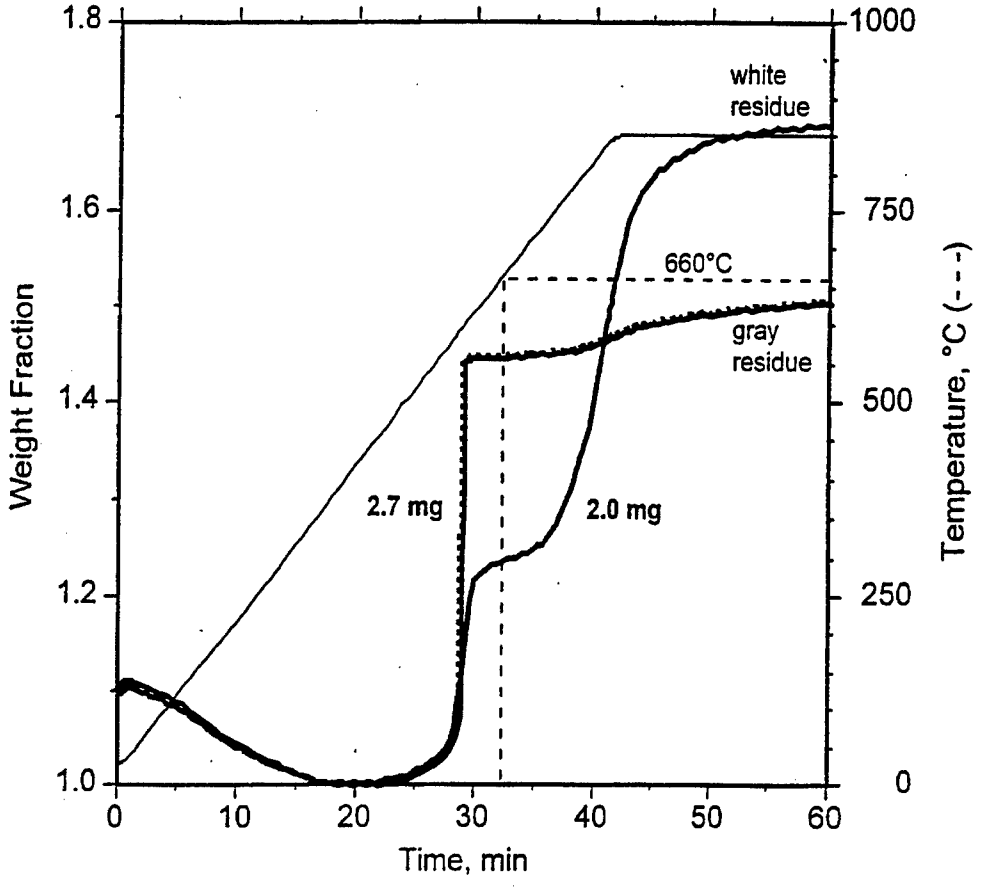


FIG. 4. TGA of aluminum powder CL-B in air showing ignition. Samples were heated at 20°C/min to 850°C, then held at 850°C. The sample weight was normalized to the minimum weight.

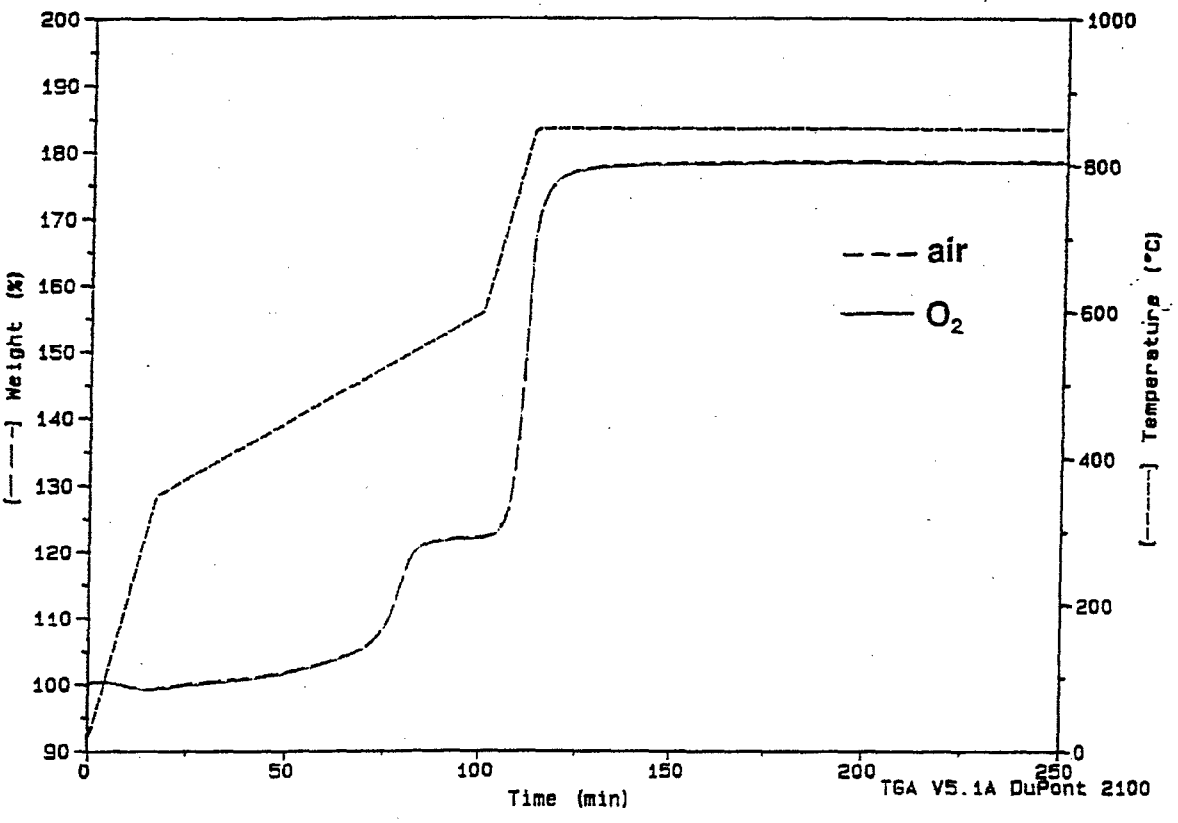


FIG. 5. TGA of aluminum powder CL-35 undergoing oxidation in air and oxygen atmospheres.

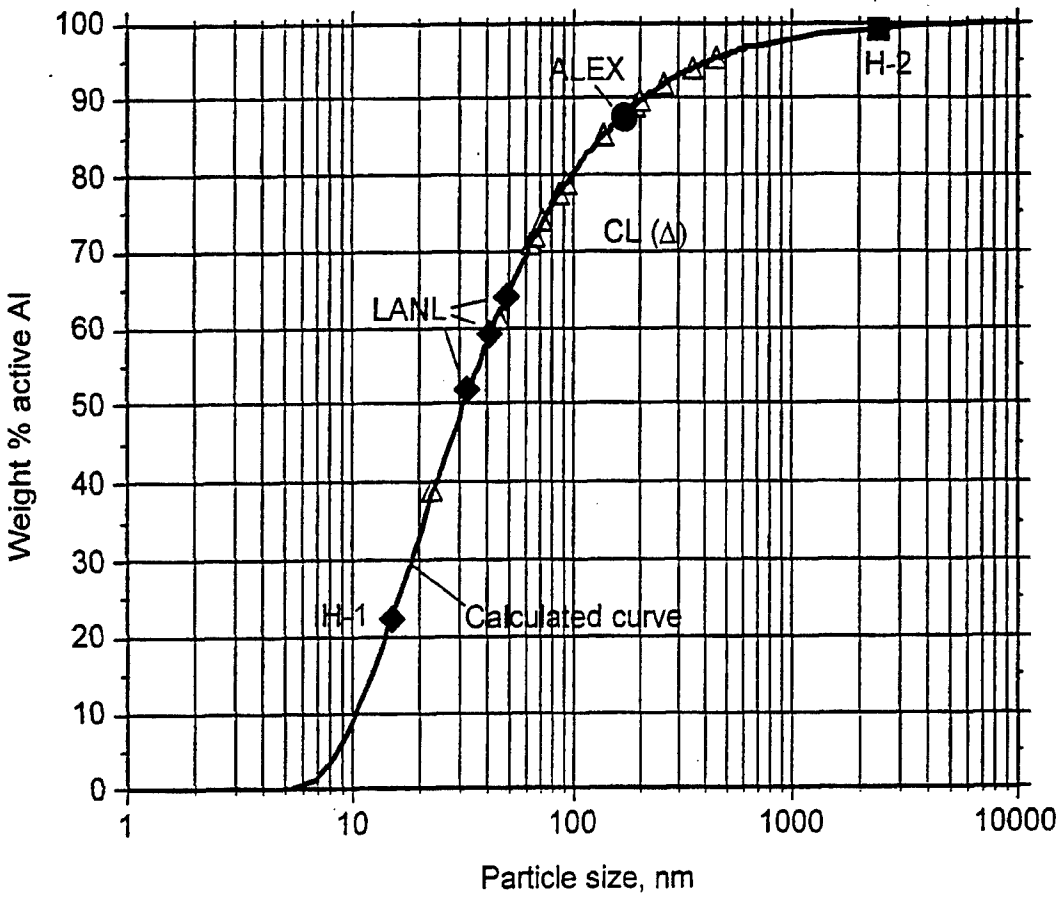


FIG. 6. Calculated weight percent of active aluminum as a function of particle size assuming spherical particles with a 2.5 nm oxide thickness.

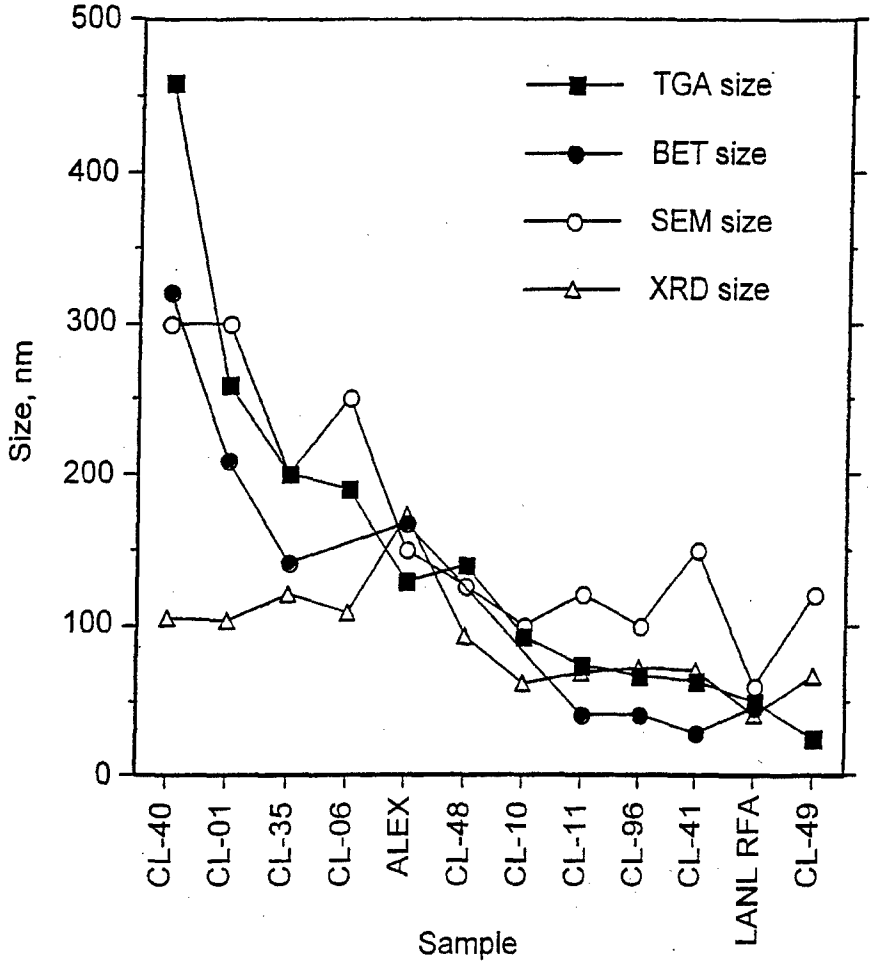


FIG. 7. Comparison of particle and crystallite sizes obtained from TGA, BET, SEM, and XRD analysis.

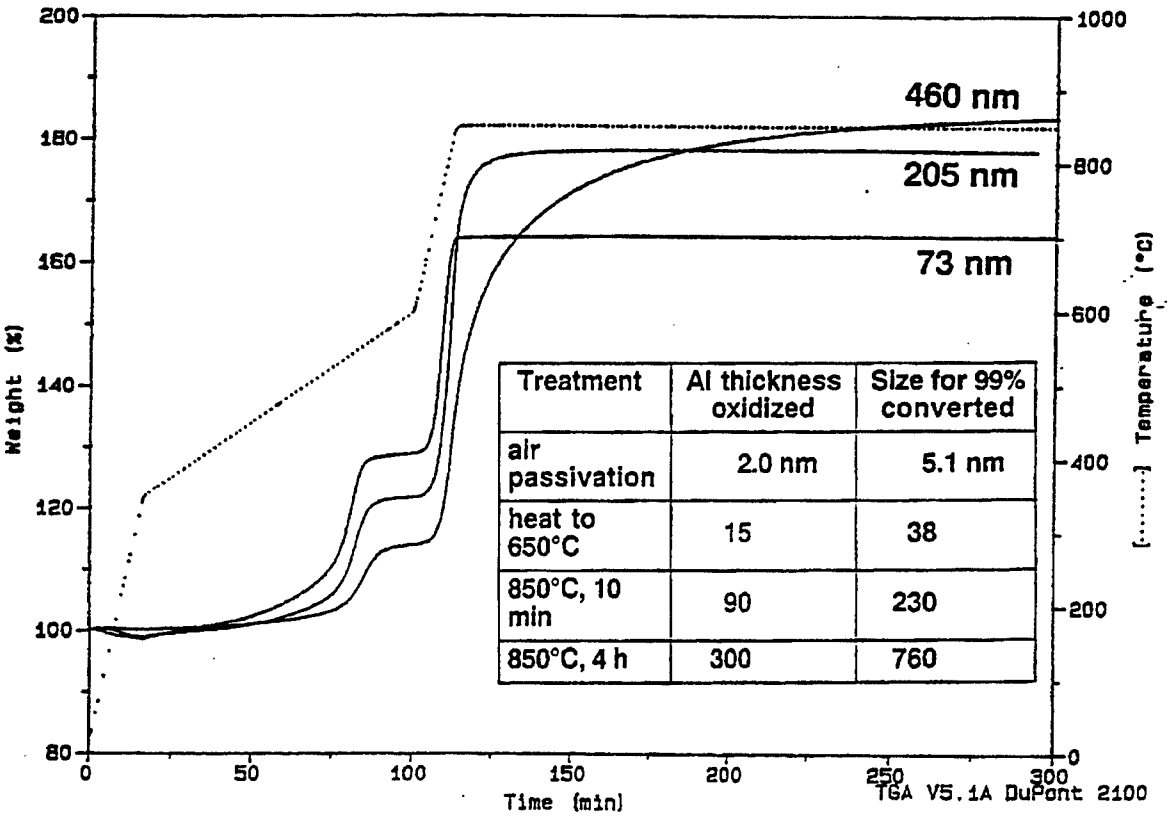


| Treatment | Al thickness oxidized | Size for 99% converted |
|---|---|---|
| air passivation | 2.0 nm | 5.1 nm |
| heat to 650°C | 15 | 38 |
| 850°C, 10 min | 90 | 230 |
| 850°C, 4 h | 300 | 760 |

FIG. 8. TGA of aluminum powders CL-40 (460 nm TGA size), CL-35 (201 nm), and CL-11 (73 nm) in air. The table gives an interpretation of the oxidation process in terms of the thickness of aluminum oxidized for various thermal treatments.

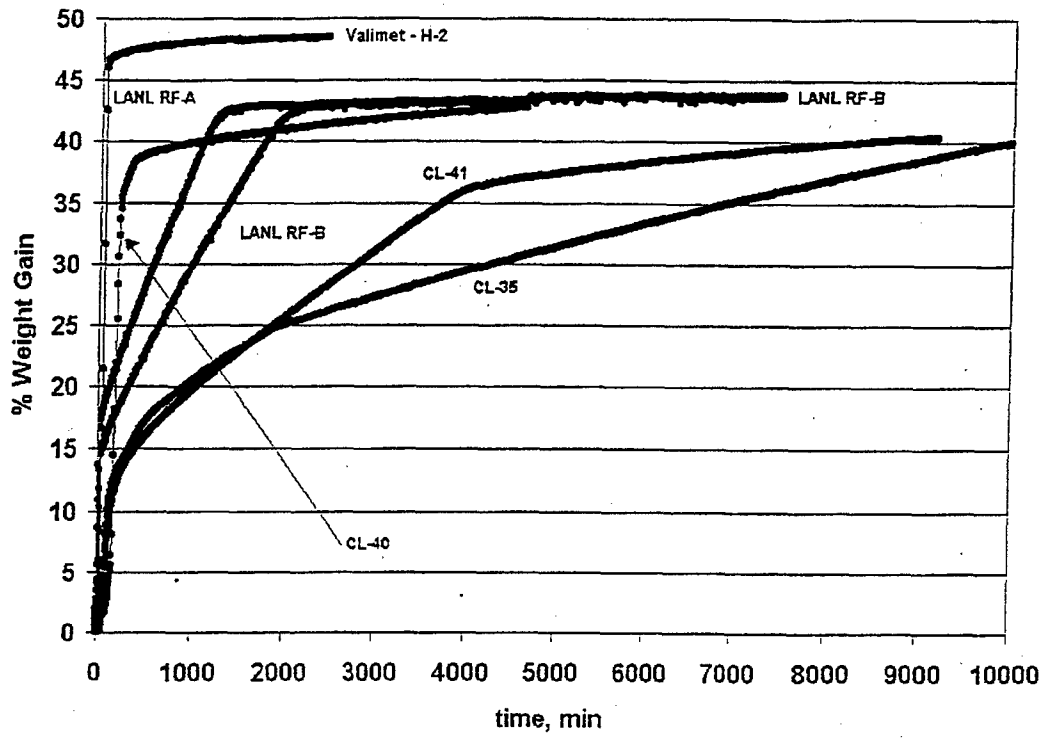


FIG. 9. TGA of aluminum powder reaction with nitrogen at 600°C.

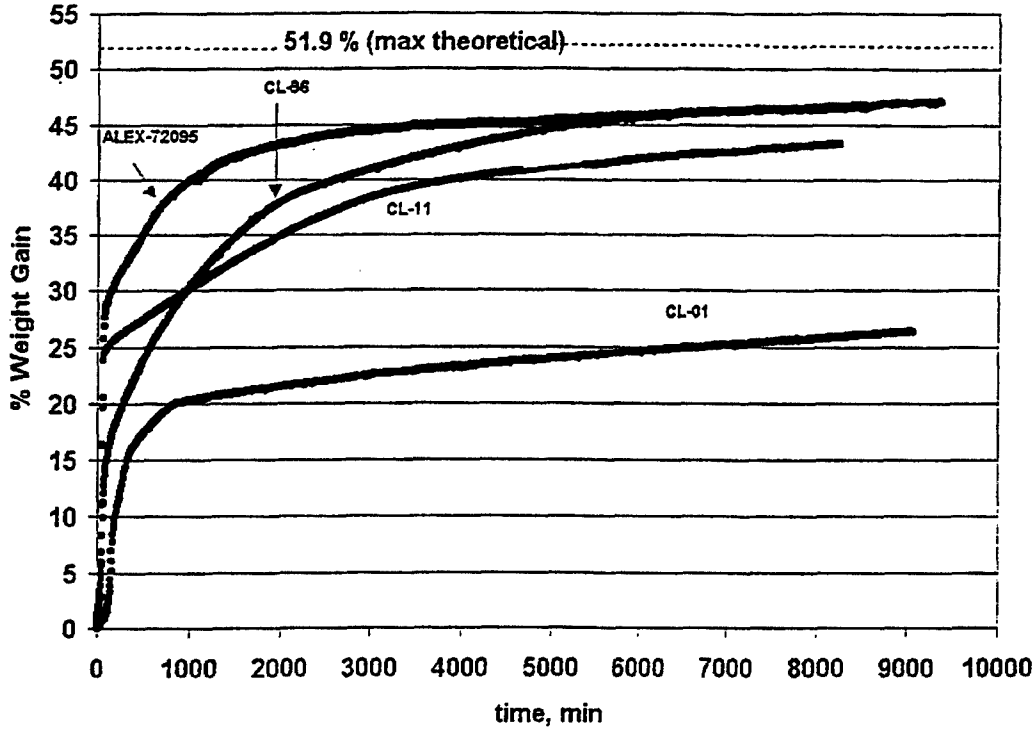


FIG. 10. TGA of aluminum powder reaction with nitrogen at 600°C.

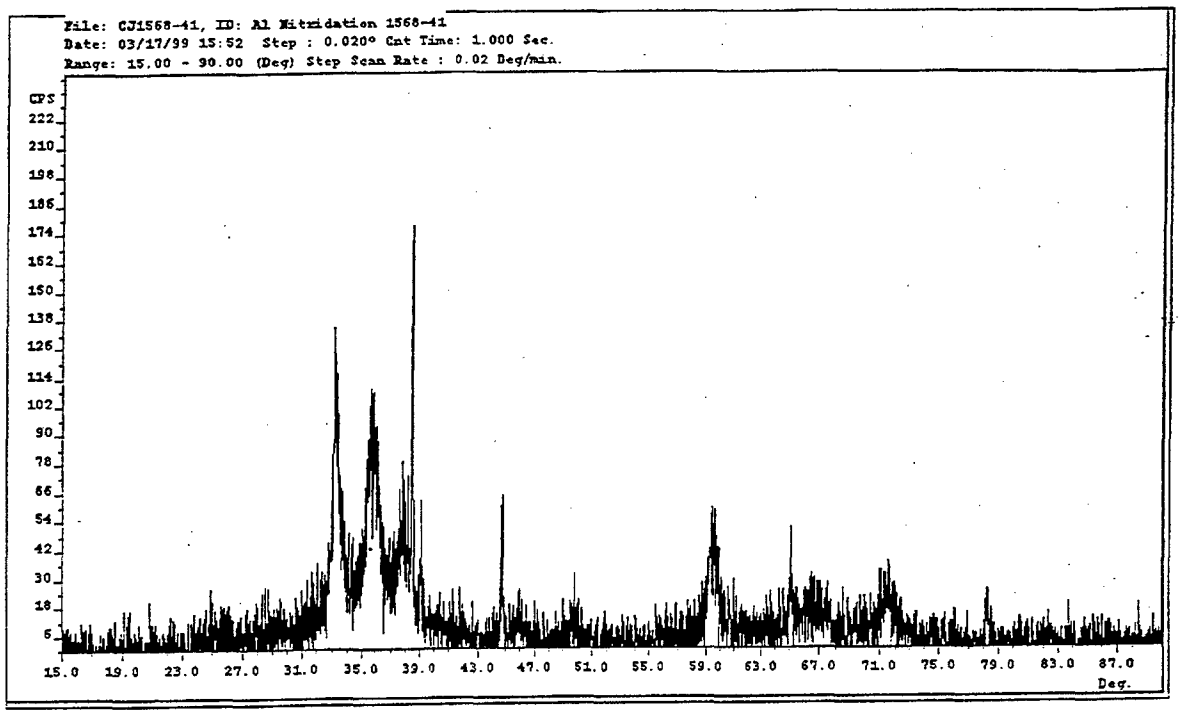


FIG. 11. X-ray diffraction of nitrided aluminum powder CL-41.